ADVANCED MATERIALS TECHNOLOGIES
www.advmattechnol.de

Single Molecule with a Large Transistor – SiMoT cytokine IL-6 Detection Benchmarked against a Chemiluminescent Ultrasensitive Immunoassay Array

Cecilia Scandurra, Kim Björkström, Lucia Sarcina, Anna Imbriano, Cinzia Di Franco, Ronald Österbacka, Paolo Bollella, Gaetano Scamarcio, Luisa Torsi, and Eleonora Macchia**

Early diagnosis and efficient treatments of oncological, neurological, inflammatory, and infectious diseases rely more and more on ultrasensitive detection of protein markers; the ultimate limit is a reliable immunoassay capable of single-protein detection. Among protein biomarkers, cytokines play a key role in clinical diagnosis as they are involved in developing many complex diseases and disorders, such as chronic inflammatory diseases including metabolic syndrome, neurodegenerative diseases, and cardiovascular diseases, along with autoimmune diseases and cancer. Herein, the improvement of a Single Molecule with Transistor (SiMoT) is reported based on an electrolyte-gated organic field-effect transistor applied for the detection of cytokine IL-6 in blood serum, reaching a limit-of-detection (LOD) of 1 ± 1 protein in a sample of 0.1 mL. The analytical performance levels are benchmarked against the Simoa Planar Array SP-X technology, a benchtop chemiluminescent array. After comprehensive optimization, Simoa SP-X by using a multivariate experimental design approach exhibits a LOD 10^3 higher than SiMoT. The proposed SiMoT electronic assay is label-free, fast (30 min), and selective, paving the way for an ultra-sensitive point-of-care immunoassay platform enabling presymptomatic disease diagnosis.

1. Introduction

Identifying proteins, peptides, and genomic biomarkers at the single molecule limit of detection is gaining momentum, as it will enable the early diagnosis of progressive, life-threatening, and life-quality-affecting diseases. From this perspective, developing more sensitive and reliable analytical biosensors can trigger great progress in biomedical research and clinical practice. Indeed, such systems' availability will allow clinicians to track many diseases at the earliest possible stage, increasing the chances of defeating them. Molecular technologies, such as Next-Generation Sequencing (NGS),[1] are able to sequence genomic markers at the single-copy level, triggering very high diagnostic sensitivity and specificity. However, technologies capable of detecting protein or peptide markers at the single-molecule level are still lacking. This is reflected in the fact that less than 20% of the human proteome is known, while thousands of human genomes have been sequenced.[2,3] In this perspective, a huge effort has been undertaken by Quanterix, introducing a micro-beads-based technology named Single-Molecule-Array, Simoa,[4] proving for the first time that detection limits of specific proteins into the low femtogram (fg) mL^{-1} (≈1–10 × 10^{-18} M, aM) range can be useful in oncology, neurology, inflammation, and infectious diseases.[5–7] Recently,

C. Scandurra, L. Sarcina, A. Imbriano, C. Di Franco, P. Bollella, L. Torsi
Dipartimento di Chimica
Università degli Studi di Bari "Aldo Moro"
Bari 70125, Italy
E-mail: luisa.torsi@uniba.it

C. Scandurra, A. Imbriano, P. Bollella, L. Torsi, E. Macchia
Centre for Colloid and Surface Science – CSGI Unit of University of Bari
Università degli Studi di Bari "Aldo Moro"
Bari 70125, Italy
E-mail: eleonora.macchia@uniba.it

The ORCID identification number(s) for the author(s) of this article can be found under https://doi.org/10.1002/admt.202201910.

DOI: 10.1002/admt.202201910

K. Björkström, R. Österbacka, L. Torsi, E. Macchia
The Faculty of Science and Engineering
Åbo Akademi University
Turku 20500, Finland

G. Scamarcio
Dipartimento Interateneo di Fisica
Università degli Studi di Bari Aldo Moro
Bari 70125, Italy

E. Macchia
Dipartimento di Farmacia-Scienze del Farmaco
Università degli Studi di Bari "Aldo Moro"
Bari 70125, Italy

the Simoa Planar Array benchtop technology (SP-X System)[8] based on a digitalized ELISA has been developed by Quanterix, being faster and less expensive than the Simoa beads-based technology. The Simoa SP-X technology can detect protein markers with LODs in the sub-femtomolar (10^{-15} M) range, which corresponds to 10^5–10^6 proteins in a sample volume of 0.1 mL, hence being sensitive to a lesser extent than NGS. Such femtomolar sensitivity relies on printing highly packed capture antibodies with a density of 10^3 μm^{-2} onto detection spots holding an area of 0.2 mm^2.[9–11] Remarkably, the elicited technologies are label-needing, requiring more steps and, hence, more time-consuming than label-free ones. These platforms are opening to the widespread use of personalized and precision medicine in everyday clinical practice. Yet, the drawbacks are that the assays do not reach the single-molecule limit for protein detection, and the labeling step contributes to the long time-to-results (several hours at minimum) and costs. Furthermore, none of them can simultaneously assay both proteins and genomic markers.

The emerging Single-Molecule with a large Transistor (SiMoT) technology[12] represents the latest development in ultrasensitive bioelectronic detection, involving the assay of biomarkers, both genetic (DNA, RNA) and proteins, at 10–20 zM (10^{-21} M) limit-of-detection. This means that one molecule is included in a sampled volume of 0.1 mL. This promising technology is based on an Electrolyte-gated field effect transistor (EG-FET)[13] encompassing a large-area (μm^2–mm^2 wide) detecting interface hosting 10^{11}–10^{12} cm^2 biorecognition elements. Notably, SiMoT is a label-free technology, indeed the output signal is directly related to a variation in the electrostatics of the immunocomplex established upon the interaction between the biomarker and its recognition element. As extensively reported in the literature, the SiMoT technology can detect both proteins (i.e. IgG, IgM, HIV-p24, and CRP),[12,14–17] and genomic markers[18–20] also in both buffered solutions and real serum at the physical limit. Moreover, the covid virus[21] and *Xylella fastidiosa* bacterium[22] have been detected at the single entity level with such technology. Those studies pave the way toward developing ultra-sensitive, fast, highly reliable, and low-cost diagnostic systems for diagnosing diseases like tumors, viral and bacterial infections early.

Moreover, bioelectronic sensors offer many relevant advantages over optical systems in biosensing applications. Indeed, electronic devices are generally label-free, fast, and easier to operate, being the perfect candidate for developing point-of-care testing. The acquired data also conveniently support the transfer and archiving into a cloud system for remote processing. Such an occurrence will put a clinician in the condition to provide an immediate clinical assessment while in a remote connection.

In this study, the detection of cytokine interleukin-6 (IL-6) has been achieved with the SiMoT technology, reaching a LOD down to the physical limit in human blood serum. In particular, cytokines are one of the main signaling molecules in charge of regulating the immune system. Their concentration changes upon infection, inflammation, or other immune response activation, thus being important biomarkers for various diseases. In particular, it has been recently demonstrated that the level of IL-6 in human blood serum can be correlated to HIV infection at significantly higher concentrations in samples collected from infected patients.[23] Importantly, the detection of these cytokines is usually accomplished only in the acute disease state when they reach measurable concentrations.[24] This usually takes place well after the appearance of clinical symptoms. Therefore, developing an ultrasensitive assay for cytokine detection is desirable to enable pre-symptomatic disease diagnosis. Here, single-molecule detection of IL-6 has been accomplished in blood serum with SiMoT technology and benchmarked against Simoa SP-X assay. To this aim, a user-customizable Simoa SP-X Homebrew assay has been optimized by means of an experimental design approach, and a limit of detection of 57 aM (10^{-18} M) has been obtained. Instead, the assay performed with the SiMoT device showed a limit of detection of 20 zM (10^{-21} M), which means detecting 1 ± 1 molecule in the sampled volume of 0.1 mL. This is obtained by means of a sensing gate electrode covered by highly packed anti-IL6 capture antibodies, at a density of 10^3 μm^{-2}, comparable to the Simoa assay. This SiMoT label-free assay is performed through the exposure of the bio-modified gate electrode to 0.1 mL of the blood serum samples to be analyzed. Moreover, to prove the selectivity of the assay, negative control experiments have been accomplished. These experiments involved a gate electrode merely covered by bovine serum albumin, exposed to the very same blood serum samples containing the specie under investigation. There should be noticed that the overall SiMoT assay is faster than the Simoa assay with time-to-results as low as 30 min.

2. Results

2.1. Simoa SP-X Assay for IL-6

The user-customizable Simoa SP-X Homebrew assay, combining contact printing technology with anchor antibody/peptide tag pairs, has been used to detect human Interleukin 6 (IL-6) in blood serum, aiming at benchmarking the Single-molecule with a large Transistor (SiMoT) technology. **Figure 1**A illustrates the main steps of the IL-6 Simoa SP-X assay. To perform the Simoa assay, the initial steps of the procedure are very much like those involved in conventional ELISA sandwiches.[14] Indeed, the Simoa assay encompasses a 96-well ELISA plate, each hosting 12 distinct circular spots, 600 μm in diameter.[8] The anti-IL6 capture antibodies' immobilization occurs through a peptide-tag coupling the selected biorecognition elements with the anchor antibodies printed with high density on specific circular spots. The IL-6 analyte is sandwiched between the peptide-tagged capture and biotinylated detector antibodies. In this study, IL-6 standard solutions, prepared in phosphate buffer saline (PBS, ionic strength 163 mM and pH 7.4) with concentrations ranging from 14 aM (0.3 fg mL^{-1}) to 14 pM (300 pg mL^{-1}), have been assayed. The target analyte was captured at the spot hosting the anti-IL6 capture antibodies. After the incubation step in the analyte solutions, the workflow proceeds with the subsequent exposure to the anti-IL6 detector antibodies labeled with biotin, forming sandwich immunocomplexes with the capture antibody-antigen complexes. Afterward, the plate is washed to remove unreacted antibodies and incubated with SA-HRP to label the immunocomplexes with enzymes. Eventually, luminol and H_2O_2 are

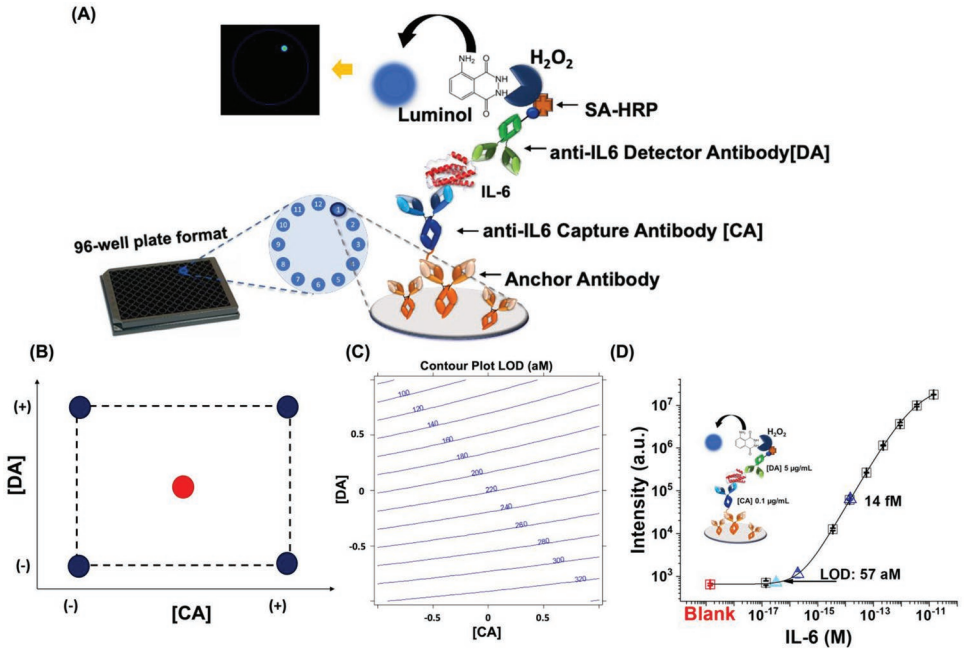

Figure 1. A) Workflow of the Simoa homebrew assay developed for the detection of the IL-6 target molecule. B) Graphical representation of the experimental domain used to develop a 2^2-factorial design. C) Isoresponse contour plot of the LOD response of the 2^2 factorial design. D) Calibration curve for optimized IL-6 assay registered with 0.1 µg mL^{-1} of anti-IL6 capture antibody and 5 µg mL^{-1} of anti-IL6 detector antibodies. IL-6 standard solutions prepared in PBS with concertation ranging from 14 aM to 14 pM have been assayed and are given as black hollow squares. Error bars are shown for two replicate measurements of IL-6 sensing (black squares) and 6 replicate measurements of blank (red square). The modeling (black solid curve) has been performed with an analytical model based on a 5-Parameter logistic equation. The triangles are relevant to the endogenous content of IL-6 measured in serum. The dark-blue hollow triangle is relevant to the serum sample 1:4 in PBS, while the light green triangles are the serum samples diluted by the standard 10-fold dilution method in PBS, ranging from 14 aM to 14 fM.

incubated in each well. Consequently, the enzyme-substrate reaction yields light emitted locally from the immunocomplexes. The intensity of the signal is directly proportional to the concentration of analyte in the analyzed solution and imaged on a CCD camera.

The sensitivity of the Simoa SP-X homebrew assay against IL-6 analyte has been optimized through an experimental design approach, encompassing two factors: the concentrations of the anti-IL6 capture and detector antibodies. Based on previous studies,[4,25] a typical experimental setting encompassing anti-IL6 capture and detector antibodies' concentrations ranging from 0.1 to 5 µg mL^{-1} has been selected as an experimental domain. The graphical representation of the experimental domain explored by the 2^2 factorial design is schematically depicted in Figure 1B, where the capture ([CA]) and detector antibodies ([DA]) concentration have been coded at low and high levels, namely −1 and +1, corresponding to 0.1 to 5 µg mL^{-1} respectively. Therefore, considering the geometrical representation of the experimental domain, the 2^2 factorial design explores the corner of a square, allowing to simultaneously vary both variables under investigation. The output of the experiment performed at the corners of the experimental domain, marked by the black points in Figure 1B, has been used to develop a linear model correlating the LOD, taken as the response of the model, with the two variables. Therefore, the following mathematical model has been implemented

$$\mathrm{LOD} = b_0 + b_1[\mathrm{CA}] + b_2[\mathrm{DA}] + b_{12}[\mathrm{CA}][\mathrm{DA}] \quad (1)$$

encompassing constant term b_0, two linear terms, and one two-term interaction that explains possible interactions between the concentration of capture and detector antibodies. The LOD of the assays has been computed as the concentration providing a response equal to $I_{\mathrm{blank}} \pm k\sigma$,

where I_{blank} is the average CCD image intensity of the blank experiment plus 3 times (k) the standard deviation of the noise (σ).[26,27] Four assays, each one in duplicate, were performed to estimate the coefficients of the model, with four degrees of freedom left to define the statistical significance of the model. In addition, two experiments were performed at the center point, shown as a red dot in Figure 1B, corresponding to a concentration of 2.5 µg mL^{-1} for both anti-IL6 capture and detector antibodies, to assess the model's prediction capability. For each assay, the dose-response curves were registered in duplicate, incubating the 8 rows of the microtiter plate with IL6 standard solutions ranging from 14 aM to 14 pM. Moreover, 6 wells of the assay were used to measure the blank signal, resulting in six replicates of the noise level. The multilinear regression coefficients of the model reported in Equation (1) have been determined along with their significance to elucidate the effect of the capture and detector antibodies concentrations, obtaining the following values:

$$\mathrm{LOD}\,(aM) = 218 + 21[\mathrm{CA}]^{(*)} - 112[\mathrm{DA}]^{(*)} + 10[\mathrm{CA}][\mathrm{DA}]^{(***)} \quad (2)$$

where the significance level is indicated according to the usual convention: $*p < 0.05$, $**p < 0.01$, $***p < 0.001$. The terms of the model are all significant terms, although the linear terms

of (DA) hold an absolute value larger than the others. The large coefficient of (DA) indicates that by increasing the concentration of the detector antibody, a decrease in the LOD of the assay is registered, and therefore better results are obtained by increasing this concentration. Indeed, the coefficient of the linear term of (DA) is negative, and since the LOD has to be minimized, it can be said that the assay's sensitivity improves working with a higher concentration of detector antibodies. Moreover, since the coefficient for each term represents the change in the mean response associated with an increase of one coded unit in that term, while the other terms are kept constant, it can be noted that by increasing the capture antibody concentration from 0.1 to 5 μg mL^{-1}, an increase in the LOD of 21 aM has been registered. To validate the model, the predicted response at the center point, namely the assay performed with 2.5 μg mL^{-1} for both concentrations of the capture and detector antibodies, has been compared with the experimental value. The predicted LOD value in the center point is 218 aM (4.6 fg mL^{-1}), while the experimental value is 238 ± 64 aM (5.0 ± 1.3 fg mL^{-1}), where the error has been computed as the experimental pooled standard deviation with four degrees of freedom. Therefore, the experimental value of the LOD measured at the center point is not significantly different from the predicted value. Thus, the model is validated and accepted in the whole experimental domain. The isoresponse contour plot, reported in Figure 1C, provides essential information about the interactions between the two variables (CA) and (DA). The contour plot shows parallel isoresponse lines, indicating a linear model without main interactions among the two variables. Moreover, the contour plot in Figure 1C clearly shows that the best condition in the explored experimental domain corresponds to a higher detector antibody concentration, while an increase in the capture antibody concentration does not lead to an improvement in sensitivity. Indeed, the anti-IL6 antibody footprint occupies a surface of ≈300 nm^2,[12] and thus ≈10^9 anti-IL6 can be hosted on the 600 μm^2 pre-spotted area of the microtiter plate wells. The anti-IL6 is thus packed on the spot of the Simoa SP-X plate at a density of 3×10^3 μm^{-2}.[25] Considering an incubation volume of 50 μL for the capture antibody solution, a minimum concentration of 30 pM, corresponding to 4.5 ng mL^{-1}, is necessary to fully cover the Simoa SP-X spot. A further increase of the capture antibody concentration does not improve the anti-IL6 surface coverage, and thus in the assay binding efficacy. Therefore, the best conditions to perform the IL-6 assay have been settled at concentrations of 0.1 and 5 μg mL^{-1} for the capture and detector antibodies respectively, to enhance the assay sensitivity while minimizing the cost of the assay. In Figure 1D, the calibration curve registered for the IL-6 assay encompassing the optimized experimental condition is reported. The black squares are relevant to the average of the exposure to IL-6 analyte standard solutions evaluated with two replicates, while the red square is the average of the signal of the blanks over six replicated experiments. The black line represents the curve fit, being a 5-Parameter Logistic (5PL) based on the following Equation:

$$I = a + \frac{d}{\left(1 + \left(\frac{x}{c}\right)^b\right)^e} \quad (3)$$

where x is the IL-6 concentration, while I is the CCD image intensity, expressed in arbitrary units. The equation parameters a and d are respectively the initial response for $x = 0$ and the maximum response of the curve, b is defined as the Hill Coefficient, c is the inflection point of the curve, and e is the non-symmetry factor. The fitting procedure was repeated several times, and the coefficients were adjusted depending on the residual errors in the previous iteration. Remarkably, a LOD as low as (57 ± 26) aM (1.1 ± 0.5 fg mL^{-1}) has been achieved, being one order of magnitude lower than the LOD obtained with commercially available Simoa kit for IL-6 detection, namely (1.5 ± 0.8) fM (31 ± 17 fg mL^{-1}).[8,28–30] The optimized experimental setting achieved with the experimental design has been used to develop the assay to measure IL-6 in blood serum samples from a human donor. The initially sampled serum fluids were assayed by Simoa (find details in Experimental Section), then tenfold standard dilutions in PBS were produced from these samples. The samples were assayed in duplicate at each dilution. The intensity of the CCD camera signal is reported in Figure 1D as blue hollow triangles. Remarkably, the maximum concentration of IL-6 in the blood serum sample assessed by Simoa is (14 ± 0.5) fM (294 ± 10 fg mL^{-1}). The sample encompassing a nominal IL-6 concentration of 140 aM is above the LOD level of the Simoa assay, returning a concentration of (193 ± 68) aM (4.0 ± 1.4 fg mL^{-1}). However, the samples with nominal ligand concentrations of 14 aM and 140 zM fall below the LOD, returning a negative response of the Simoa assay.

2.2. IL-6 SiMoT Assay

The SiMoT device structure is shown in **Figure 2**A. This comprises a Si/SiO_2 substrate on which the interdigitated source (S) and drain (D) electrodes are deposited and covered by the p-type organic semiconductor (P3HT). The third electrode, the gate (G), controls the conductivity of the electronic channel, by means of the HPLC-grade water, that acts as an electrolyte medium. The SiMoT technology uses two circular gate electrodes (≈0.2 cm^2), one used as a reference for the overall measurements and the other is the sensing bio-modified gate. They have the same geometry and they are both manufactured on a PEN substrate by e-beam evaporation (with two layer Ti/Au, 5 nm/50 nm) and they are alternatively measured. In detail during the analysis, the reference gold gate is stably positioned in the electrolyte well over the channel area, and it is used to monitor the device's stability during the whole assay. Instead, on the sensing gate electrode trillions of anti-IL6 antibodies are deposited. The very same antibodies used as capture antibodies in the Simoa assay are used, to highly specifically bind the IL-6. The biorecognition elements were immobilized on the sensing gate surfaces via a self-assembled monolayer (SAM) approach. Both 3-mercaptopropionic acid and 11-mercaptoundecanoic acid are mixed and used to define the chem-SAMs on the gold electrode surface. The well-known EDC/sulfo-NHS chemistry has been used to covalently bind the biological recognition elements to the SAM. Indeed, the capture antibodies can be bound through their amine groups to the activated carboxylic moieties of the chem-SAM. After the anti-IL6 has been coupled, the activated but non-reacted acidic functionalities can

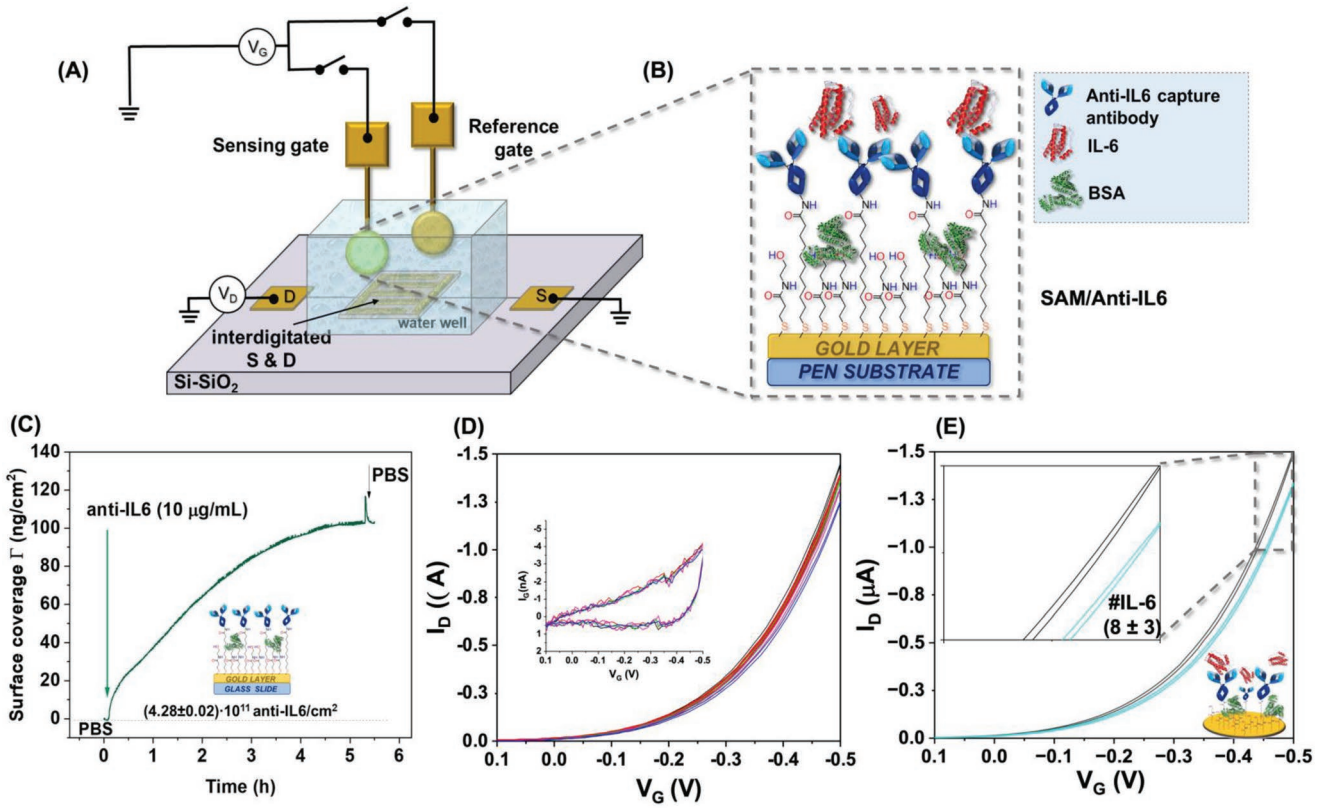

Figure 2. A) SiMoT device structure encompassing interdigitated source (S) and drain (D) electrodes covered by Poly(3-hexylthiophene-2,5-diyl) – P3HT. Two gate electrodes are used: a bare gold reference gate and a biofunctionalized one. B) Schematic representation of the covalent biofunctionalization strategy pursued to immobilize anti-IL6 antibodies on the sensing gate electrode. C) SPR sensogram of the anti-IL6 covalent immobilization through mixed-SAM on the gold SPR slide. Two areas were sampled on the surface in each experiment, shown as blue and curves. D) SiMoT sensing transfer characteristics (I_D vs V_G at $V_D = -0.4$ V). The black curve corresponds to the anti-IL6 functionalized gate incubated in the sole PBS solution. The same gate is further exposed, in sequence, to PBS standard solutions of IL-6 at concentrations of 14 zM (red-curve), 1.4 aM (green-curve), 14 aM (magenta-curve), 140 fM (blue-curve). The gate leakage current I_G for the anti-IL6 sensing gate incubated in PBS and in IL-6 standard solutions is shown as an inset. E) SiMoT sensing transfer characteristics (I_D vs V_G at $V_D = -0.4$ V). The curve in black is the trace recorded for the anti-IL6 functionalized gate when incubated in the blank PBS solution; the cyan curve is recorded after the gate has been incubated in IL-6 dilution at nominal concentrations of 140 zM, namely (8 ± 3) IL-6 molecules in the sampled volume. A zoom into the VG range from –0.4 to –0.5 V is reported in the inset.

be saturated with ethanolamine. To complete the biofunctionalization, BSA is deposited on the electrode to prevent any non-specific binding. A scheme of the SAM gained through this protocol is reported in Figure 2B.

The biofunctionalization protocol has been monitored in situ via Surface Plasmon Resonance (SPR) characterization. To this aim, a Multi-Parameter SPR Navi 200-L apparatus in the Kretschmann configuration was used, as reported elsewhere.[31,32] An optical glass coated with a gold (≈50 nm) on chromium (≈2 nm) layer has been engaged as a semi-transparent SPR slide. The slide is modified with the mixed SAM and then allocated in the sample holder and placed into the SPR flow-through cell in which the subsequent biofunctionalization steps have been performed. The biofunctionalization protocol is monitored via the evanescent wave generated by a laser beam (λ = 670 nm) reflecting on the Au-covered optical glass.[33,34] The gold exposed area, ≈0.4 cm^2, was simultaneously examined by two SPR laser sources that hit the sensor at two points (3 mm apart), to evaluate the uniformity of the antibody layer deposited on the sensor surface. In this SPR setup, static injections are used. In detail, 0.1 mL of the anti-IL6 capturing antibodies (10 µg mL^{-1}) phosphate buffer solution (I_s = 163 mM, pH 7.4)are injected over the SAM-modified gold surface. The optical signal changes occurring as the biolayer was deposited were recorded as a function of time and shown as the green and blue curves in Figure 2C. The almost identical traces served to assess the homogeneity of the anti-IL6 surface coverage. To observe a plateau upon the binging of anti-IL6, the solution was let to interact with the activated SAM for up to 5 h. The increase of the optical signal reported in Figure 2C, indicates that a film of anti-IL6 forms on the slide in 4 h, reaching 95% of the coverage.

An anti-IL6 surface coverage of 103.2 ± 0.4 ng cm^{-2}, corresponding to (4.28 ± 0.02) × 10^{11} molecules × cm^{-2} was computed by using the de Feijter's equation.[17,18,31,32] Hence, the anti-IL6, deposited from a 10 µg mL^{-1} solution, is packed at a density of 4 × 10^3 μm^{-2}, comparable to the capture antibody density achieved with the Simoa technology. The sensing gate, biofunctionalized with anti-IL6 according to the protocol monitored with SPR, has been engaged in the SiMoT assay to detect human IL-6. To this aim, the sensing gate is immersed for ten minutes into an incubation well hosting 0.1 mL of the blood

serum samples or the IL-6 standard solutions in PBS, that is the high ionic strength (162 mM) media. The sensing gate is then washed and positioned in the measuring SiMoT well with low ionic strength (≈5 μM) deionized (DI) water to maximize the Debye's length and hence the output electronic sensing response. The binding event produced a variation of the source-drain current (I_{DS}) of the SiMoT device, by capacitively coupling the sensing gate to the transistor channel, ascribable to a shift of the *sensing* gate work function.[12,35] The bare gold reference gate, stably positioned over the SiMoT electronic channel, controls the device's stability during the whole assay. Remarkably, the bare gold electrode engaged in the SiMoT technology does not act as an ideally non-polarizable reference electrode (such as an Ag/AgCl one), which is required to operate amperometric sensors.[36] In contrast, the SiMoT technology foresees a potentiometric measurement, since no I_G current flows. The transistor transfer characteristics, namely the I_D as a function of the gate voltage (V_G) at a fixed source-drain voltage (V_{DS}) of −0.4 V, measured with the sensing gate assaying IL-6 standard solutions, are reported in Figure 2D. The baseline (I_0) is reported as a black curve, and it is measured after the sensing gate was incubated in a bare PBS (I_s = 162 mM) solution. Then, the same sensing gate is incubated in 0.1 mL of IL-6 PBS spiked solution at a concentration of 14 zM (1.4×10^{-20} M), which means 1 ± 1 target molecule can be found in the assayed volume, where the indetermination is the Poisson sampling error.[12,20] Thus, upon the binding of a single IL-6 molecule a new trace is recorded. Here, in Figure 2D, the red curve is related to the signal level *I*, which is measured in the SiMoT device after binding the target species. As shown in Figure 2D, the sensing gate is then tested against the exposure to increasing concentrations of IL-6 spiked PBS solutions at a concentration of 1.4 aM (green-curve), 14 aM (magenta-curve), and 140 fM (blue-curve). In the inset of Figure 2D, the curves corresponding to the gate leakage currents (I_G) of the device are shown, which are always at least three orders of magnitude lower than I_D. Thus, no faradaic activity can be evidenced by the I_G curve of the sensing gate, proving that mild electrochemical processes have been prevented by fine-tuning the inspected gate voltage window. Moreover, Figure 2D also shows no correlation between the I_G current and the ligand concentration. These are compelling evidence, proving that the field-effect induced current I_D provides a capacity-coupled related sensing response. In particular, when the gate voltage is applied, the gate modulates, according to its electrochemical potential, the conduction in the EG-FET semiconductor through the charge double layer (CDL) at the gate–membrane/electrolyte interface. The electrolyte/semiconductor interfaces hold a second CDL, that capacitively couples to the gate/electrolyte one. Those CDLs are built via transient ionic currents (non-faradaic) measured as an I_G gate-leakage ionic current that extinguishes once the electrostatic equilibrium is reached. Relevantly, to prevent any electronic-faradaic current, the gate voltage is swept across ranges where no redox reactions occur. Thus, if no leakage gate current I_G flows between the gate and the source/drain electrodes, the zero-current (I_G = 0) equilibrium potential governing a Nernstian behavior is satisfied.[36] These working conditions mean that the EG-FETs operate as a potentiometric sensor, where the capacitive coupling between the gate/membrane and the semiconductor channel transduces the gate/membrane electrochemical potential shift by modulating the I_D current.

In Figure 2E the baseline current level is shown as a black curve, and it is compared to the transfer characteristic recorded after the *sensing* gate is incubated in the IL-6 standard solution at a nominal concentration of 140 zM (cyan-curve), corresponding to 8 ± 3 target molecules in the assayed volume of 0.1 mL. A large current decrease is observed as well as a shift of the transfer characteristic toward more negative V_G. The transfer characteristics are analyzed by taking into account the relative shift of the measured current (*I*), compared to the baseline (I_0), namely $(\Delta I/I_0) = [(I - I_0)/I_0]$, at the maximum transconductance, and this was taken as the SiMoT response.[15,17,22] Also, as validation methodology for the assay, the I_D current recorded with the bare gold reference gate were monitored for the whole sensing assay, and these variation in the current relative shift remained below 5%. In **Figure 3**A the dose-response curves of the ($\Delta I/I_0$) SiMoT assay for both the sensing (black squares) and the negative control (red circles) experiments carried out in IL-6 spiked PBS solutions are reported. The sensing experiment encompasses a sensing gate biofunctionalized with anti-IL6 antibodies, while the negative control experiment has been conducted with a bare BSA biofunctionalized gate. The modeling of the SiMoT sensing response (solid black curve) was carried out utilizing an analytical model based on Poisson distribution probability[16] encompassing the following five parameters logistic equation:

$$\frac{\Delta I}{I_0} = a + \frac{d}{\left(1 + \left(\frac{x}{c}\right)^b\right)^e} \tag{4}$$

where x is the IL-6 concentration, while $\Delta I/I_0$ is the SiMoT response. The fitting parameters engaged in Equation (4) are the same used to fit the Simoa response reported in Equation (3) (vide supra). This accounts for the occurrence of a few binding events, as described in detail elsewhere.[22] The assay noise level is given from the negative control experiment, resulting in $(\Delta I/I_0) = 0.03 \pm 0.02$. The LOD level, taken as the concentration corresponding to the noise average level plus three times its standard deviation,[26] is as low as 20 zM (2×10^{-20} M). The sampled solutions are all 0.1 mL hence the LOD corresponds to 1 ± 1 target molecule. Therefore, according to Poisson's distribution, there is a 64% probability that a 20 zM solution host at least one molecule.

In Figure 3B the SiMoT and Simoa assays are compared for the experiments performed with human blood samples from a healthy donor. Here, the human serum was first assayed by Simoa, and from this, 10-fold standard diluted solutions in PBS were produced. Each dilution was tested twice, taking 0.1 mL for each assay. The normalized $(\Delta I/I_0)$ (black hollow squares) and intensity of the chemiluminescent signal collected by the Simoa CCD camera (grey hollow triangles) are plotted. The noise levels, computed as the average response of the BSA biofunctionalized gate assaying whole human blood serum, resulted in a $(\Delta I/I_0)$ of 0.11. This leads to a LOD of 1 ± 1 target molecule in 0.1 mL. Remarkably, a recent study has demonstrated that a single antigen (out of a few) in a 0.1 mL sampled volume, acting as a Browning particle obeying Einstein's

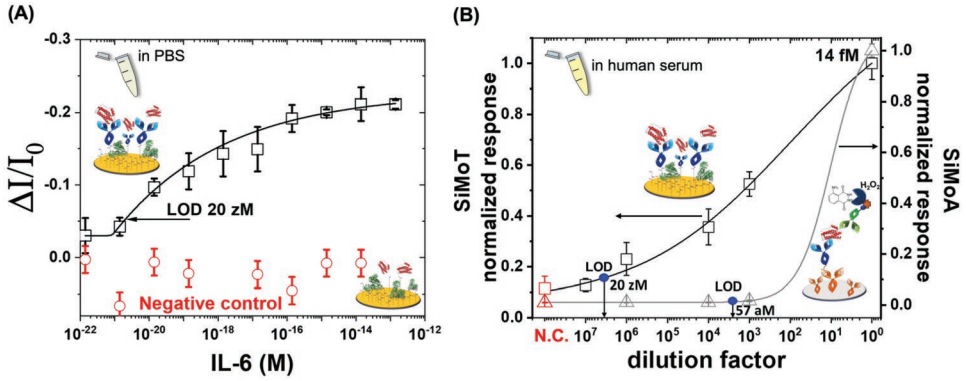

Figure 3. A) IL-6 dose-curves obtained with the electronic SiMoT assay, performed in PBS standard solutions in a range of concentration of 14 zM–140 fM. The data determined with the sensing gate biofunctionalized with anti-IL6 and incubated into the IL-6-standard solutions are reported as black hollow squares, while the response measured from the negative control experiments, encompassing a bare BSA biofunctionalized sensing gate, are shown as red hallow circles. Error bars over three replicates are set as one standard deviation. The modeling (black solid curve) has been performed with an analytical model based on a 5-Parameter logistic. The LOD, taken as the average of the control experiment data (noise level) plus three times the standard deviation, is equal to 1 ± 1 IL-6 in 0.1 mL. B) The SiMoT and the Simoa dose curves were measured on the same blood serum samples from a healthy donor. The maximum concentration of IL-6 assessed by Simoa is 14 fM. The other points are relevant to tenfold standard dilutions of the blood serum in PBS reference fluid. The red hollow square is relevant to the SiMoT negative control experiment, performed using a bare BSA functionalized gate exposed to the undiluted bold serum sample, while the red hollow triangle is the blank experiment of the Simoa assay. The data have been acquired from nominally identical samples and the error bars are taken as one standard deviation. On the left, the ($\Delta I/I_0$) normalized data of SiMoT response are shown, while on the right, the Simoa values of the intensity registered with the CCD camera for each assayed sample are reported. Also in this case the modeling (black solid curve) has been performed with an analytical model based on a 4-Parameter logistic equation based on the same set of parameters derived from the calibration dose curve in PBS.

diffusion theory, can strike with a very high probability, a 0.2 cm^2 large-area gate functionalized with 10^{11} antibodies, within a few minutes.[37] Moreover, a recent study has directly measured through Kelvin probe force microscopy (KPFM) the surface potential changes associated with antigen–antibody bindings at a large-area biofunctionalized metal surface.[38] In particular, KPFM data have directly and independently demonstrated that the binding of less than 10 ligands to an equal number of biorecognition elements is capable to shift the surface potential of 10^8 antibodies that are highly packed on a 90×90 μm^2 wide gate. Meaning that the electrostatic interactions spread on highly packed layers of capturing antibodies, as the one deposited on the gate surface, allow the propagation of the electrostatic change of the single capturing antibody through the whole surface.

The curves for this set of measurements were fitted by means of a 5-parameter logistic equation, as previously mentioned, which is based on the same parameters resulting from the calibration dose curve obtained in the experiments involving IL-6 standard solutions in PBS, and a good agreement with the experimental data was found. For the assay conducted with the Simoa platform, the LOD was evaluated as the concentration corresponding to the average signal of the blank plus three times its standard deviation. A value of 57 aM was found, corresponding to $(1.7 \pm 0.4) \times 10^3$ target molecules in 0.05 mL incubation volume. Hence the LOD obtained with SiMoT technology is three orders of magnitude lower than the one achieved with the Simoa SP-X system.

There should be highlighted that the SiMoT technology is a time-to-result and label-free technique in which the assay can be performed in ≈30 min, instead, the Simoa label-needing technology requires at least 4.5 h analysis because of the multi-steps needed to complete the assay.

3. Conclusion

In conclusion, the analytical performance of the SiMoT device capable of electronic label-free detection of IL-6 in human blood serum at a LOD of 1 ± 1 target molecule in 0.1 mL, is benchmarked toward a commercially available chemiluminescence-based Simoa SP-X IL-6 assay. This is performed utilizing a millimeter-wide (0.2 cm^2) gate bearing a layer of 10^{11} anti-IL6 capture antibodies packed at the same density of 10^3 μm^{-2} engaged in the Simoa assay. The sensing experiment can be performed by the direct incubation of the gate electrode for 10 minutes into reduced volume (0.1 mL) of blood serum, whose IL-6 content has independently been assayed by Simoa. By means of the SiMoT technology, a label-free, fast, and cost-effective assay is feasible, reaching detection limits about three orders of magnate lower than Simoa. Negative control experiments involved a bare BSA biofunctionalized gate exposed to whole human blood serum. The results obtained with this proposed assay unfold the development of a point-of-care immunometric sensor, that can perform ultra-sensitive analysis even for the large-scale screening of a plethora of progressive diseases.

4. Experimental Section

Materials: The Simoa Planar array homebrew starter kit was purchased from Quanterix. Those kit encompassed the monoclonal Anti-human Interleukin 6 (anti-IL6) Capture Antibody in an aqueous buffered solution, with sodium azide preservative (Molecular weight $M_W \approx 150$ kDa), the monoclonal Anti-human Interleukin 6 (anti-IL6) Detector Antibody in aqueous buffered solution, with sodium azide preservative (Molecular weight $M_W \approx 150$ kDa), and lyophilized human Interleukin-6 antigen (IL6) affinity ligand. PBS pH 7.2 and ionic strength 163 mM, Tween 20, Sulfosuccinimidyl 4-(N-maleimidomethy) cyclohexane-1-carboxylate

(Sulfo-SMCC), 1 M Tris HCl pH 7.4, NHS-PEG4-Biotin, Streptavidin Horseradish Peroxidase (SA-HRP), Horseradish Peroxidase Substrate-(SuperSignal Luminol), sample diluent (Phosphate buffer with BSA and sodium azide as preservative) were purchased from Quanterix. Universal ELISA plates pre-spotted with an anchor (immobilized protein) were purchased from Quanterix and stored at 2–8 °C. Anti-IL6 capture antibodies against the IL-6 target proteins were exchanged into PBS and incubated for 30 min at 23 °C with Sulfo-SMCC. Maleimide-activated capture antibodies were subsequently incubated with a peptide tag purchased from Quanterix and used without further purification at a 1.2 mg mL^{-1} concentration for 30 min at 23 °C. The maleimide-activated antibody with the peptide occurred through a cysteine group on the peptide. Peptide labeled capture antibodies were purified via dialysis in PBS using an Amicon Ultra-0.5 Centrifugal Filter Devices. The capture antibodies solution concentration was adjusted to 0.25 mg mL^{-1} in 1 × PBS, 4% BSA, 0.1% sodium azide, and stored at 2–8 °C until ready to run the assay. According to standard protocols, anti-IL6 detection antibodies were exchanged into PBS and then biotinylated using NHS-PEG4-Biotin (50X molar excess of biotin to antibody). The biotinylated antibodies were purified from excess biotin by dialysis into PBS using an Amicon filter. IL-6 calibrator antigen stocks were prepared through serial dilution using the sample diluent. Human serum samples were obtained from blood samples collected from a different healthy donor (age between 18 and 60, Research Donors Ltd of London (UK)) and centrifugated at 10000 × *g* for 5 min and successively diluted 1:4 with PBS, before the Simoa and SiMoT assays.

Simoa Assay Development: Anchor antibodies pre-spotted arrays on dried microtiter plates were washed with 25 X Wash Buffer (Tris-based buffer with Tween 20 detergent) on a Simoa washer (Quanterix Corporation) prior to use it. The peptide-tagged anti-IL6 capture antibody solution in the sample diluent, with a concentration in the range of 0.1 to 5 μg mL^{-1}, with a volume of 50 μL was added to each well of the washed plates. The plates were incubated for 30 min at 23 °C while shaken at 525 r.p.m. on an orbital plate shaker. Those shaker parameters were used for all subsequent incubation steps. When the peptide-labeled anti-IL6 capture antibody immobilization was accomplished, the plates were washed, and a volume of 50 μL of IL-6 calibrator solutions with concentration ranging from 14 aM (0.3 fg mL^{-1}) to 14 pM (300 pg mL^{-1}) was added into each well. Plates were incubated for 120 min before washing and incubating with 50 μL of biotinylated anti-IL6 detection antibodies for 30 min. Plates were rewashed, and 50 μL of streptavidin-horseradish peroxidase (SA-HRP) enzyme conjugate was added to each well and incubated for 30 min. Finally, the plates were washed before adding 50 μL of luminol and hydrogen peroxide to each well. Plates were imaged on the Simoa SP-X (Quanterix Corp.). Fluorescence images were acquired (577 nm excitation, 620 nm emission) and recorded using a CCD camera.[16]

Design of Experiments: A replicated, two-factors, full factorial design was implemented to optimize the Simoa assay. The factors examined were the concentration of anti-IL6 capture antibody (CA) and detection antibody (DA), coded with X_1 and X_2 variables, respectively. Following a two-level design, these variables were set at a low and high level, coded as –1 and +1. For each factor, the levels of 0.1 and 5 μg mL^{-1} were selected for both capture and detection antibodies. The concentration range selected for the capture and detection antibodies was customary to develop ELISA and Simoa SP-X assays.[8,25,39,40] The experimental matrix is given in **Table 1**.

The LOD of each assay, computed according to the IUPAC definition,[41] was used as the response to the full factorial design. In addition, the LOD at the center point in duplicate was evaluated and used to validate the linear model with interactions provided by the factorial design. Multilinear regression was performed. The full factorial 2^2 design and the validation were performed using CAT (Chemometric Agile Tool) open-source software.[42]

Samples from Human Serum: Human serum samples from blood samples collected from a different healthy donor were first centrifugated at 10 000 × *g* for 5 min and successively first diluted 1:4 with PBS. The serum samples were diluted (by the standard tenfold dilution method) in PBS. The endogenous IL6 concentration in each sample was quantified by Simoa assay,[8] using Simoa Planar Array Homebrew Starter Kit (Product number 100–0464). The SiMoT technology also analyzed the same samples.

Table 1. Experimental matrix, experimental plan, and responses of the 2^2 Full Factorial Design, along with the center point used for the model validation.

(CA)	(DA)	(CA) [μg mL^{-1}]	(DA) [μg mL^{-1}]	LOD [aM]
–1	–1	0.1	0.1	487
–1	–1	0.1	0.1	319
1	–1	5	0.1	395
1	–1	5	0.1	378
–1	+1	0.1	5	56
–1	+1	0.1	5	64
1	1	5	5	137
1	1	5	5	149

Electrolyte-Gated Organic Thin-Film Transistor Fabrication: EG-FETs with spin-coated organic semiconductors[43,44] were prepared on a Si/SiO_2 substrate as previously reported.[12] The sensing and reference gold PEN gates were fabricated as previously reported.[45]

Gate Bio-Functionalization and Measurements Protocol: The gate biofunctionalization protocol was optimized and described in detail elsewhere and herein adapted for anti-IL6.[12,46] The SiMoT device was stabilized before performing sensing experiments, according to the protocol defined and validated elsewhere.[19,20]

SiMoT Assay Measurement Protocol: The SiMoT device was stabilized before performing sensing experiments, according to the protocol defined and validated elsewhere.[19,20] The protocol described in the following section was used for the sensing measurements. In detail, each sensing gate modified with anti-IL6 was let to interact for 10 min with 100 μl of the reference fluid, and then properly rinsed with HPLC water and positioned on top of the SiMoT electrolyte cell. Then, an iteration of 20 transfer characteristics was acquired to establish the initial I_0 baseline level. The sensing gate was then incubated in 100 μl of the IL-6 standard solutions in PBS (ionic strength 162 mM and pH 7.4) at concentrations ranging from 14 zM (1.4×10^{-20} M) to 140 fM (1.4×10^{-13} M) for 10 min. After each incubation in the IL-6 containing solutions, the sensing gate was washed carefully in HPLC grade water to remove any excess of species not bound to the biofunctionalized surface, and a further set of SiMoT transfer characteristic was recorded, thus providing the current signal *I* from each concentration. In the case of negative control experiments, a gate surface biofunctionalized merely with BSA (0.1 mg mL^{-1}) was used to acquire a control dose curve involving the exposure to IL-6 of this BSA-passivated electrode. These control experiments were also used to define the LOD level of the bioelectronic assay. Also, in the experiments involving the samples from human serum, in the SiMoT assay, negative control experiment the BSA-functionalized gates were exposed to an undiluted blood serum sample.

The IL-6 standard solutions in PBS were prepared by a serial dilution process according to the following equation: $c_2 = c_1 \times V_1 / V_2 = k \times c_1$. Here c_1 and c_2 are the ligand concentrations in the stock and in the diluted solution, respectively, while V_1 and V_2 are the corresponding solution volumes and $k = V_1 / V_2$ is the dilution factor. As customary, the former dilution was the stock solution for the subsequent dilution in the series. Standard ten-fold serial dilutions starting from concentrated analytes´ mother solution were performed. On each concentration of the standard solutions, the absolute uncertainty was calculated as the propagation error of the dilution factor, while the uncertainty of the volume, given by the supplier company of the pipettes used, was 1%. This value of the uncertainty of the volume considers both random and systematic errors in pipetting. The nominal number of IL-6 at each concentration was given by the equation $c \times V \times N_A$, where c is the IL-6

concentration, *V* is the volume of the standard PBS solution in which the gate is incubated (100 µL) and N_A is the Avogadro number. The error associated with the sampling procedure could be estimated according to Poisson's distribution. The total uncertainty of the ligand concentration was evaluated as the square root of the sum of the squares (RSS) of the dilution (σ_D) and Poisson's (σ_P) errors. This means that the 100 µl of human serum solutions, in which the sensing gate was incubated, hosted a number of IL-6 ligands ranging from 1 ± 1 molecules (14 zM) to ($8 \times 10^6 \pm 3 \times 10^3$) molecules (140 fM). For monitoring the device stability during the assay, the time required for each incubation of the reference gate in the fluids was used to measure 5 repeated transfer characteristics, delayed by 10 s, in the same voltage range used for the sensing gate. All data acquired during the experiments were plotted and analyzed using the Origin2018 software.

Acknowledgements

H2020 – Electronic Smart Systems – SiMBiT: Single-molecule bioelectronic smart system array for clinical testing (Grant agreement ID: 824946), NoOne-A binary sensor with a single-molecule digit to discriminate biofluids enclosing zero or at least one biomarker, ERC Stg2021, GA:101040383, Biosensori analitici usa-e getta a base di transistori organici auto-alimentati per la rivelazione di biomarcatori proteomici alla singola molecola per la diagnostica decentrata dell'HIV (6CDD3786); Research for Innovation REFIN—Regione Puglia POR PUGLIA FESR-FSE 2014/2020, PMGB—Sviluppo di piattaforme meccatroniche, genomiche e bioinformatiche per l'oncologia di precisione—ARS01_01195-PON "RICERCA E INNOVAZIONE" 2014–2020, Åbo Akademi University CoE "Bioelectronic activation of cell functions", Svenska Tekniska Vetenskapsakademien i Finland, and CSGI are acknowledged for partial financial support.

Open access funding provided by Universita degli Studi di Bari Aldo Moro within the CRUI-CARE agreement.

Conflict of Interest

The authors declare no conflict of interest.

Data Availability Statement

The data that support the findings of this study are openly available in https://ida.fairdata.fi/s/NOT_FOR_PUBLICATION_Af5XREMArsD2.

Keywords

cytokine IL-6 detections, electrolyte-gated organic field-effect transistors, sandwich immunoassays, Simoa SP-X technology, single-molecule assay with a large transistor (SiMoT)

Received: November 10, 2022
Revised: February 26, 2023
Published online: March 22, 2023

[1] J. M. Rothberg, W. Hinz, T. M. Rearick, J. Schultz, W. Mileski, M. Davey, J. H. Leamon, K. Johnson, M. J. Milgrew, M. Edwards, J. Hoon, J. F. Simons, D. Marran, J. W. Myers, J. F. Davidson, A. Branting, J. R. Nobile, B. P. Puc, D. Light, T. A. Clark, M. Huber, J. T. Branciforte, I. B. Stoner, S. E. Cawley, M. Lyons, Y. Fu, N. Homer, M. Sedova, X. Miao, B. Reed, et al., *Nature* **2011**, *475*, 348.
[2] A. A. Deniz, *J. Mol. Biol.* **2016**, *428*, 301.
[3] S. Kumar, D. Clarke, M. B. Gerstein, *Proc. Natl. Acad. Sci. USA* **2019**, *116*, 18962.
[4] D. M. Rissin, C. W. Kan, T. G. Campbell, S. C. Howes, D. R. Fournier, L. Song, T. Piech, P. P. Patel, L. Chang, A. J. Rivnak, E. P. Ferrell, J. D. Randall, G. K. Provuncher, D. R. Walt, D. C. Duffy, *Nat. Biotechnol.* **2010**, *28*, 595.
[5] X. Wang, L. Cohen, J. Wang, D. R. Walt, *J. Am. Chem. Soc.* **2018**, *140*, 18132.
[6] S. K. Fischer, A. Joyce, M. Spengler, T. Y. Yang, Y. Zhuang, M. S. Fjording, A. Mikulskis, *AAPS J.* **2015**, *17*, 93.
[7] D. M. Rissin, D. R. Walt, *J. Am. Chem. Soc.* **2006**, *6*, 520.
[8] C. I. Tobos, S. Kim, D. M. Rissin, J. M. Johnson, S. Douglas, S. Yan, S. Nie, B. Rice, K. J. Sung, H. D. Sikes, D. C. Duffy, *J. Immunol. Methods* **2019**, *474*, 112643.
[9] B. Spurrier, P. Honkanen, A. Holway, K. Kumamoto, M. Terashima, S. Takenoshita, G. Wakabayashi, J. Austin, S. Nishizuka, *Biotechnol. Adv.* **2008**, *26*, 361.
[10] V. Romanov, S. N. Davidoff, A. R. Miles, D. W. Grainger, B. K. Gale, B. D. Brooks, *Analyst* **2014**, *139*, 1303.
[11] SP-X Imaging and Analysis SystemTM, https://www.quanterix.com/instruments/the-sp-x-imaging-and-analysis-system/ (accessed: July 2022).
[12] E. Macchia, K. Manoli, B. Holzer, C. Di Franco, M. Ghittorelli, F. Torricelli, D. Alberga, G. F. Mangiatordi, G. Palazzo, G. Scamarcio, L. Torsi, *Nat. Commun.* **2018**, *9*, 3223.
[13] F. Torricelli, D. Z. Adrahtas, Z. Bao, M. Berggren, F. Biscarini, A. Bonfiglio, C. A. Bortolotti, C. D. Frisbie, E. Macchia, G. G. Malliaras, I. McCulloch, M. Moser, T. Q. Nguyen, R. M. Owens, A. Salleo, A. Spanu, L. Torsi, *Nat. Rev. Methods Primers* **2021**, *1*, 66.
[14] E. Macchia, K. Manoli, C. Di Franco, G. Scamarcio, L. Torsi, *Anal. Bioanal. Chem.* **2020**, *412*, 5005.
[15] S. K. Sailapu, E. Macchia, I. Merino-Jimenez, J. P. Esquivel, L. Sarcina, G. Scamarcio, S. D. Minteer, L. Torsi, N. Sabaté, *Biosens. Bioelectron.* **2020**, *156*, 112103.
[16] E. Macchia, A. Tiwari, K. Manoli, B. Holzer, N. Ditaranto, N. Picca, R. A. Cioffi, C. Di Franco, G. Scamarcio, G. Palazzo, L. Torsi, *Chem. Mater.* **2019**, *31*, 6476.
[17] E. Macchia, K. Manoli, B. Holzer, C. Di Franco, R. A. Picca, N. Cioffi, G. Scamarcio, G. Palazzo, L. Torsi, *Anal. Bioanal. Chem.* **2019**, *411*, 4899.
[18] L. Sarcina, L. Torsi, R. A. Picca, K. Manoli, E. Macchia, *Sensors* **2020**, *20*, 3678.
[19] E. Macchia, L. Sarcina, C. Driescher, Z. Gounani, A. Tewari, R. Osterbacka, G. Palazzo, A. Tricase, Z. M. Kovacs Vajna, F. Viola, F. Modena, M. Caironi, F. Torricelli, I. Esposito, L. Torsi, *Adv. Electron. Mater.* **2021**, *7*, 2100304.
[20] L. Sarcina, F. Viola, F. Modena, R. A. Picca, P. Bollella, C. Di Franco, N. Cioffi, M. Caironi, R. Österbacka, I. Esposito, G. Scamarcio, L. Torsi, F. Torricelli, E. Macchia, *Anal. Bioanal. Chem.* **2022**, *414*, 5657.
[21] E. Macchia, Z. M. Kovács-Vajna, D. Loconsole, L. Sarcina, M. Redolfi, M. Chironna, F. Torricelli, L. Torsi, *Sci. Adv.* **2022**, *8*, abo0881.
[22] L. Sarcina, E. Macchia, G. Loconsole, G. D'Attoma, P. Bollella, M. Catacchio, F. Leonetti, C. Di Franco, V. Elicio, G. Scamarcio, G. Palazzo, D. Boscia, P. Saldarelli, L. Torsi, *Adv. Sci.* **2022**, *9*, 2203900.
[23] J. M. Haissman, L. S. Vestergaard, S. Sembuche, C. Erikstrup, B. Mmbando, S. Mtullu, M. M. Lemnge, J. Gerstoft, H. Ullum, *Infection* **2009**, *52*, 493.
[24] T. Hirano, *Int. Immunol.* **2021**, *33*, 127.
[25] C. Scandurra, P. Bollella, R. Österbacka, F. Leonetti, E. Macchia, L. Torsi, *Adv. Sens. Res.* **2022**, *1*, 2200009.

[26] M. Thompson, S. L. R. Ellison, R. Wood, *Pure Appl. Chem.* **2002**, *74*, 835.
[27] L. Torsi, M. Magliulo, K. Manoli, G. Palazzo, *Chem. Soc. Rev.* **2013**, *42*, 8612.
[28] Simoa Planar Array Homebrew Assay Kit, https://www.quanterix.com/whitepapers-appnotes/simoatm-planar-array-homebrew-assay-kit/ (accessed: July 2022).
[29] C. I. Tobos, A. J. Sheehan, D. C. Duffy, D. M. Rissin, *Anal. Chem.* **2020**, *92*, 5613.
[30] K. B. Casaletto, F. M. Elahi, R. Fitch, S. Walters, E. Fox, A. M. Staffaroni, B. Bettcher, H. Zetterberg, A. Karydas, J. C. Rojas, A. L. Boxer, J. H. Kramer, *Cytokine* **2018**, *111*, 481.
[31] L. Sarcina, E. Macchia, G. Loconsole, G. D'Attoma, P. Saldarelli, V. Elicio, G. Palazzo, L. Torsi, *Adv. Nanobiomed. Res.* **2021**, *1*, 2100043.
[32] L. Sarcina, G. F. Mangiatordi, F. Torricelli, P. Bollella, Z. Gounani, R. Österbacka, E. Macchia, L. Torsi, *Biosensors* **2021**, *11*, 180.
[33] E. T. Gedig, *Handbook of Surface Plasmon Resonance*, 2nd ed., The Royal Society Of Chemistry, Cambridge **2017**.
[34] J. Homola, *Chem. Rev.* **2008**, *108*, 462.
[35] C. Di Franco, E. Macchia, N. Di Taranto, A. Khaliq, L. Torsi, G. Scamarcio, *Adv. Mater. Interfaces* **2023**, *10*, 2201829.
[36] E. MacChia, R. A. Picca, K. Manoli, C. Di Franco, D. Blasi, L. Sarcina, N. Ditaranto, N. Cioffi, R. Österbacka, G. Scamarcio, F. Torricelli, L. Torsi, *Mater. Horiz.* **2020**, *7*, 999.
[37] E. Macchia, L. De Caro, F. Torricelli, C. Di Franco, G. F. Mangiatordi, G. Scamarcio, L. Torsi, *Adv. Sci.* **2022**, *9*, 2104381.
[38] C. Di Franco, E. Macchia, L. Sarcina, N. Ditaranto, A. Khaliq, L. Torsi, G. Scamarcio, *Adv. Mater. Interfaces* **2022**, *10*, 2201829.
[39] G. S. Sittampalam, W. C. Smith, T. W. Miyakawa, D. R. Smith, C. McMorris, *J. Immunol. Methods* **1996**, *190*, 151.
[40] D. Wu, M. D. Milutinovic, D. R. Walt, *Analyst* **2015**, *140*, 6277.
[41] J. Mocak, A. M. Bond, S. Mitchell, G. Scollary, A. M. Bond, *Pure Appl. Chem.* **1997**, *69*, 297.
[42] Gruppo di Chemiometria, http://www.gruppochemiometria.it/index.php/software/19-download-the-r-basedchemometric-software (accessed: September 2022).
[43] A. J. Lovinger, D. D. Davis, A. Dodabalapur, H. E. Katz, L. Torsi, *Am. Chem. Soc.* **1996**, *29*, 4952.
[44] A. J. Lovinger, D. D. Davis, R. Ruel, L. Torsi, A. Dodabalapur, H. E. Katz, *J. Mater. Res.* **1995**, *10*, 2958.
[45] D. Blasi, F. Viola, F. Modena, A. Luukkonen, E. MacChia, R. A. Picca, Z. Gounani, A. Tewari, R. Österbacka, M. Caironi, Z. M. Kovacs Vajna, G. Scamarcio, F. Torricelli, L. Torsi, *J. Mater. Chem. C* **2020**, *8*, 15312.
[46] B. Holzer, K. Manoli, N. Ditaranto, E. Macchia, A. Tiwari, C. Di Franco, G. Scamarcio, G. Palazzo, L. Torsi, *Adv. Biosyst.* **2017**, *1*, 1700055.